Supporting Information

Live-cell labeling of endogenous proteins with nanometer precision by transduced nanobodies

Alina Klein,[a] Susanne Hank,[a] Anika Raulf,[b] Eike F. Joest,[a] Felicitas Tissen,[a] Mike Heilemann,[b] Ralph Wieneke*[a] and Robert Tampé *[ac]

[a]Institute of Biochemistry, Biocenter, and Cluster of Excellence – Macromolecular Complexes, Goethe-University Frankfurt, Max-von-Laue-Str. 9, D-60438 Frankfurt/M., Germany

[b]Institute of Physical and Theoretical Chemistry, Goethe University Frankfurt, Max-von-Laue Str. 7, 60438 Frankfurt/Main, Germany

[c]Cluster of Excellence – Macromolecular Complexes, Goethe University Frankfurt, Max-von-Laue Str. 9, 60438 Frankfurt/Main, Germany

Table of Contents for Supporting Information

Plasmid construction.

For expression in *E. coli*, the α-GFP nanobody (Kirchhofer *et al*., 2010), equipped with a C-terminal His_6-tag for purification via metal ion affinity chromatography, was inserted into the pET21a(+) plasmid. For site-specific labeling, a free single cysteine was introduced C-terminally to the His_6-tag. The α-GFP nanobody was PCR amplified by the following primers: fw 5'-GCGCGCAAGCTT*AAGGAG*ATATACAT**ATG**CAGGTTCAGCTGGTTGAAA GCGGTGGTGCAC-3' (Hind III restriction site underlined, RBS italic, start codon bold); rev 5'-GCGCCTCGAGG**TCAGCA***GTGGTGATGGTGATGATG*GCTGCTAACGGTAACCTGGGT GCCC-3' (XhoI restriction site underlined, stop codon bold, cysteine bold and underlined, His_6-tag italic). For expression in mammalian cells, α-GFP as well as mCherry were PCR amplified and introduced into the pcDNA3.1(+) plasmid, resulting in a plasmid coding for α-$GFP^{mCherry}$. fw 5'-GCGCGCGCTAGCACC**ATG**CAGGTTCA GCTGGTTGAAAGCGG-3' (NheI restriction site underlined, start codon bold) and rev 5'-GCGCGCGGTACCGCTGCTA ACGGTAACCTGGGTGCCC-3' (Acc65I restriction site underlined) for the α-GFP nanobody and fw 5'-CGCGCGGTACC**ATG**GTGAGCAAGGGCGAG GAGCTGTTC-3' (Acc65I restriction site underlined, start codon bold) and rev 5'-GCGCGCCTCGAG**TTA** CTTGTACAGCTCG TCCATGCCGAGAG-3' (XhoI restriction site underlined, stop codon bold) for mCherry. The α-Lamin nanobody was also inserted into the pET21a(+) plasmid and equipped with a His_6-tag for purification. Using α-Lamin-EGFP as PCR template, α-Lamin was amplified, introducing a C-terminal cysteine (α-$Lamin^{His6\text{-}Cys}$), a N-terminal cysteine (^{Cys}α-$Lamin^{His6}$), or replacing serine 9 by a cysteine (α-$Lamin^{S9C\text{-}His6}$). α-$Lamin^{His6\text{-}Cys}$: fw 5'-GCGCAAGCTT*AAGGAG*ATATACAT**ATG**GCTCAGGTACAGCTGCAGGAGTCTGGAG GAGG-3' (HindIII restriction site underlined, start codon bold, RBS italic); rev 5'-GCGCCTCGAG**TTAACA***GTGGTGATGGTGATGATG*CGATATCGAATTCCTTGAGGAGA CGGTGACCTGGG-3' (XhoI restriction site underlined, stop codon bold, cysteine bold and underlined, His_6-tag italic). To attach the PelB leader sequence and the cysteine, ^{Cys}α-$Lamin^{His6}$ were amplified in consecutive extending PCRs, each of them being the template for the subsequent amplification. The rev primer 5'-GCGCGCCTCGAG**TTA***GTGGT*

*GATGGTGATGATG*GGTGGCGACCGGCCG-3' (XhoI restriction site underlined, stop codon bold, His_6-tag italic) was thereby applied in combination with the following fw primers. ^{Cys}α-Lamin^{His6}: fw1 5'-*GGATTGTTATTACTCGCGGCCCAGCCGGCC***TGT**GCTCAGGTACA GCTGCAGGAGTCTGGAGGAGG-3' (cysteine bold, part of pelB leader sequence italic), fw2 5'-GCGCGCTAGC**ATG***AAATACCTATTGCCTACGGCAGCCGCTGGATTGTTATTACTCGC GGCCCAGCCGGCC*-3' (NheI restriction site underlined, start codon bold, pelB leader sequence italic). α-Lamin$^{S9C-His6}$: fw1 5'-ATGGCTCAGGTACAGCTGCAGGAGTGTGGAGGA GGCTTGGTGCAGGCAGGGGGGTCTCTG-3', fw2 5'-*GGATTGTTATTACTCGCGGCCCAG CCGGCC*ATGGCTCAGGTACAGCTGCAGGAG**TGT**GGA-3' (cysteine bold, part of pelB leader sequence italic), fw3 5'-GCGCGCTAGC**ATG***AAATACCTATTGCCTACGGCAGCC GCTGGATTGTTATTACTCGCGGCCCAGCCGGCC*-3' (NheI restriction site underlined, start codon bold, pelB leader sequence italic). The plasmid coding for H2B^{EGFP} was obtained from Addgene (plasmid 11680). The generation of plasmids coding for core TAP1 (TAP1^{mVenus}) and ^{mEGFP}Lamin A was described previously (Kollmannsperger *et al.*, 2016; Parcej *et al.*, 2013).

Protein purification

Two different protocols were used for purification. For α-GFP$^{His6-Cys}$ and α-Lamin$^{His6-Cys}$ expressed in *E. coli* BL21 (DE3), cell pellets were resuspended in lysis buffer (20 mM Tris pH 8.0, 100 mM NaCl, 1 mM phenylmethylsulfonyl fluoride **(**PMSF), 0.5 mM β-mercaptoethanol (β-ME)), followed by sonication for cell lysis. Cell debris were pelleted by ultracentrifugation (100,000x g, 30 min, 4 °C). For metal affinity chromatography, the supernatant was incubated with 3 ml Ni-NTA Sepharose beads (GE Healthcare) in the presence of imidazole (15 mM). Afterwards, the beads were washed in purification buffer (50 mM Tris pH 8.0, 300 mM NaCl, 50 mM imidazole, 0.5 mM β-ME). His-tagged proteins were eluted by 200 mM imidazole/purification buffer. Protein concentration was determined at A_{280}. Buffer exchange to phosphate-buffered saline (PBS) containing 0.5 mM β-ME by Zeba spin desalting columns (7K) was followed by concentration via Amicon Ultra Filters

(3 K). β-ME was directly removed before labeling the nanobodies using Zeba spin desalting columns (7K). Alternatively, nanobodies expressed in *E. coli* T7 Express were purified as described above, but at pH 7.5 and without β-ME.

Protein modification

Fluorescent dyes were either attached to the engineered cysteines or to lysines (only for α-Lamin$^{His6\text{-}Cys}$). The engineered cysteines of nanobodies stored in PBS without β-ME were reduced by incubation with 15 mM TCEP for 10 min on ice with subsequent buffer exchange by Zeba spin desalting columns (7K). Cysteine labeling was conducted following two different protocols: First, nanobodies were incubated with sulfo-Cy5 (sCy5) or sulfo-Cy3 (sCy3) maleimide in PBS (pH 7.4) for 1.5 h at 4 °C. Labeling was conducted at a protein concentration of approximately 1 mg/ml with 1.2-fold molar excess of the dye. Second, buffer was exchanged to maleimide labeling buffer after TCEP reduction (100 mM KH_2PO_4 pH 6.4, 150 mM NaCl, 1 mM EDTA, 250 mM sucrose). Afterwards, the fluorophore was added in a 1.2-fold molar excess, immediately followed by neutralization to pH 7.5 using K_2HPO_4 and 1.5 h incubation at 4 °C. For lysine labeling, nanobodies in PBS (pH 7.4) were mixed 1:20 with 0.1 mM $NaHCO_3$ (pH 9.0) to achieve pH 8.3 for labeling. Next, Alexa647 NHS ester was added with a 5-fold molar excess. Labeling was performed for 1 h at 20 °C before buffer exchange and removal of excess dye with Zeba spin desalting columns (7K, Thermo Scientific). Fluorescently labeled nanobodies were analyzed by SDS-PAGE and in-gel fluorescence (Typhoon 9400 Imager; $\lambda_{ex/em}$ 630/670 nm). fNbs were finally purified by size-exclusion chromatography in PBS using a KW404-4F column (Shodex; flow rate 0.3 ml/min). All labeled nanobodies were stored in PBS at 4 °C. The nanobody-to-fluorophore ratio was determined using absorption (A_{280} for nanobodies, A_{550} for sCy3, A_{663} for ATTO655, A_{649} for sCy5) and their respective extinction coefficient ε ($0.22 \cdot 10^5$ $M^{-1} \cdot cm^{-1}$ for α-Lamin Nb, $0.27 \cdot 10^5$ $M^{-1} \cdot cm^{-1}$ for α-GFP Nb, $1.36 \cdot 10^5$ $M^{-1} \cdot cm^{-1}$ for sCy3, $1.25 \cdot 10^5$ $M^{-1} \cdot cm^{-1}$ for ATTO655, and $2.50 \cdot 10^5$ $M^{-1} \cdot cm^{-1}$ for sCy5).

Nanobody production

The nanobodies were produced in E. coli BL21 (DE3, Life technologies) or E. coli SHuffle T7 Express (New England Biolabs), whereas the latter contains a chromosomal copy of a disulfide isomerase, engineered to produce proteins with disulfide bonds in the cytosol. Both E. coli strains were transformed with the vectors, coding for α-GFP and α-Lamin nanobodies with engineered cysteines. A single colony was inoculated in LB medium containing 100 µg/ml ampicillin and 2% (w/v) glucose. After overnight incubation (37 °C for E. coli BL21 (DE3) and 30 °C for E. coli SHuffle T7 Express, 180 rpm), 1 l Lysogeny Broth (LB) medium with 100 µg/ml ampicillin was inoculated and protein expression was induced at A600 of 0.7-0.8 by 1 mM isopropyl-β-thiogalactopyranoside (IPTG, Sigma-Aldrich) and conducted for 5-20 h (30 °C, 180 rpm). After centrifugation (20 min, 4°C, 5,000x g), the cell pellets were directly used for protein purification or stored at -20 °C.

Cell culture and transfection

HeLa Kyoto cell lines were cultivated in Dulbecco's Modified Eagle Medium (DMEM) with 4.5 g/l glucose (Gibco) containing 10% (v/v) fetal calf serum (FCS, Gibco). Cells were regularly tested for Mycoplasma contamination.(Uphoff and Drexler, 2014) Cells were transiently transfected using Lipofectamine 2000 (Life technologies), following the manufacturer's instructions. For staining of fixed cells, $2 \cdot 10^4$ cells per well were seeded into 8-well on cover glass II slides (Sarstedt) and transfected at ~ 80% confluency. For cell squeezing, $8 \cdot 10^5$ cells were seeded into 6-well cell culture plates (Greiner) and transiently transfected. After transfection, cells were incubated for 12-24 h at standard cell culture conditions until experiments were performed.

Cell fixation and labeling

Cells were washed with PBS (Sigma-Aldrich), fixed with 4% formaldehyde (Roth)/PBS for 10-20 min at 20 °C and permeabilized using 0.1% Triton X-100 (Roth)/PBS (10 min, 20 °C).

After blocking with 5% (w/v) bovine serum albumin (BSA; Albumin Fraction V, Roth) in PBS for 1 h at 20 °C, cells were stained. Staining was performed with fNbs (diluted in 1% BSA/PBS) at concentrations ranging from 50 to 500 nM (indicated in each case). Subsequently, cells were washed with PBS and optionally stained with 0.1 µg/ml 4',6-diamidino-2-phenylindole (DAPI, Sigma-Aldrich) in 1% BSA/PBS for 30 min to 1 h at 20 °C. After washing with 5% BSA/PBS (3x), cells were post-fixed with 2% formaldehyde/PBS (15 min, 20 °C) and stored in PBS until imaging was performed.

Nanobody transfer by cell squeezing

Squeezing was performed using a chip with constrictions of 7 µm in diameter and 10 µm in length (CellSqueeze 10-(7)x1, SQZbiotech). In all microfluidic experiments, a cell density of $1.5 \cdot 10^6$ cells/ml in 10% (v/v) FCS/PBS was squeezed through the chip at a pressure of 30 psi. Transduction was conducted at 4 °C to block cargo uptake by endocytosis (Kollmannsperger *et al*., 2016). During squeezing, the following fNb concentrations in the surrounding buffer were used: 100-200 nM of α-GFP, 200-500 nM of α-Lamin, and 50 µg/ml of α-Vimentin. After squeezing, cells were incubated for 5 min at 4 °C to reseal the plasma membrane. Squeezed cells were washed with DMEM containing 10% FCS, seeded into 8-well on cover glass II slides (Sarstedt) or collagen-coated dishes (µ-slide 8-well, Collagen IV coverslip, ibidi) in DMEM containing 10% FCS, and cultured at 37 °C and 5% CO_2. Confocal imaging was performed 1 h and 20 h after squeezing. Squeezing experiments for live-cell protein labeling highly reproducible in at least three independent experiments for every POI.

Confocal laser scanning microscopy

Imaging was performed using the confocal laser scanning (LSM) microscope LSM880 (Zeiss) or TCS SP5 microscope (Leica) with Plan-Apochromat 63x/1.4 Oil DIC objectives. To avoid crosstalk between different fluorophores, images were acquired sequentially. The following laser lines were used for excitation: 405 nm for DAPI; 488 nm for EGFP, mEGFP,

and mVenus; 565 nm for sCy3; 633 nm for sCy5 and ATTO655. Live-cell imaging of endogenous proteins (except for dual-color imaging with ATTO488 and ATTO655) was conducted with the Airy scan detector of the LSM880 in the SR-mode. For 3D reconstructions of labeled protein networks, z-stack were recorded with the Airy scan detector (200 nm distance between stacks). For live-cell imaging, an incubation system was used to keep cells at 37 °C and supply them with 5% CO_2 during imaging. ImageJ (Girish and Vijayalakshmi, 2004), Fiji (Schindelin *et al*., 2012), and Zen 2.3 black (Carl Zeiss Jena GmbH, Germany) were used for image analysis and to analyze Pearson's coefficients from 8-11 individual cells per condition. The mean and standard deviation were calculated.

Super-resolution microscopy

For super-resolution imaging of the α-Lamin^{ATTO655} fNb in live cells, a custom-built microscope was used. Samples were illuminated with 643 nm (iBeam smart, Toptica Photonics) laser beams and a 405 nm reactivation laser (Cube 405-50C, Coherent) in total internal reflection fluorescence (TIRF) mode. The excitation light was focused on the back focal plane of a 100x oil objective (Plan Apo 100x TIRFM, NA 1.45, Olympus), mounted on an inverted microscope (Olympus IX71). The emission was recorded using an EMCCD camera (IxonUltra, Andor) with frame-transfer mode, 1x pre-amplifier gain and EM gain set to 200. For every sample, 40,000 images were recorded at a frame rate of 33 Hz. Image reconstruction was performed with rapidSTORM (Wolter *et al*., 2010) using the smooth by differences of averages option with a signal-to-noise ratio of 20, fitting only PSFs with FWHM ranging from 240-520 nm and X-Y-ratio of 0.7-1.3. The average localization precision (σ_{loc}) defined as the nearest neighbor distance in adjacent frames (Endesfelder *et al*., 2014) was calculated to 23.4 ± 8.3 nm for living and 23.2 ± 4.6 nm for fixed cells (mean and standard deviation of three individually analyzed cells, respectively) using LAMA software (Malkusch and Heilemann, 2016). The average image used for visualization of nuclear intensity profiles in Figure 3c was generated by averaging the fluorescence intensity over 100 frames and

subsequent background subtraction with a rolling ball method (20 pixel radius) in ImageJ and Fiji.

Supplemental Figures

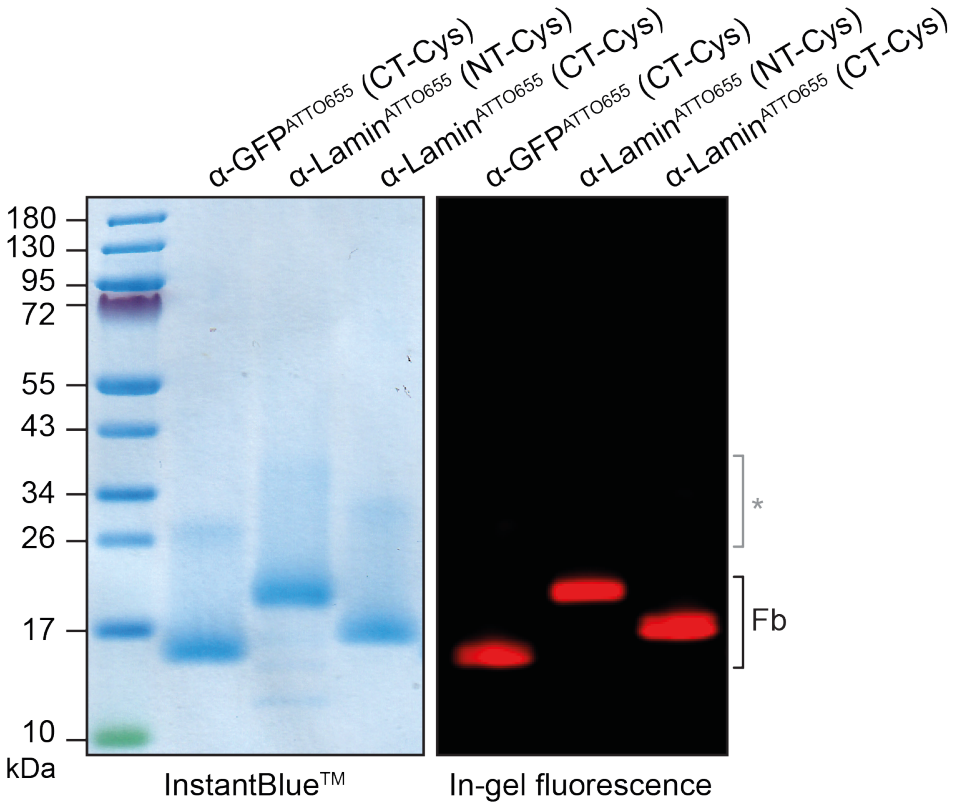

Figure S1. Site-specific fluorescent labeling of nanobodies.

Single engineered surface cysteines of nanobodies were modified with maleimide ATTO655. SDS-PAGE analysis showed covalent labeling of the engineered fNbs. Detection was performed by InstantBlue™ staining and by in-gel fluorescence with $\lambda_{ex/em}$ 630/670 nm. A minor portion of fNb dimers (*) was observed. The higher molecular weight of α-Lamin (NT-Cys) is due to an elongated linker between Nb and C-terminal His_6-tag.

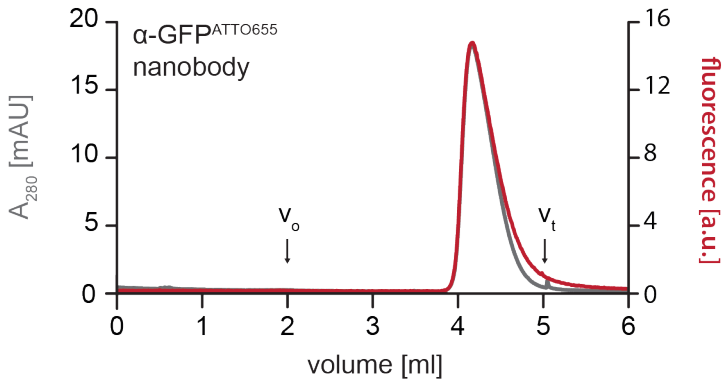

Figure S2. Analysis of site-specifically labeled α-GFP^{ATTO655} fNbs.

Size-exclusion chromatography (SEC) of the site-specifically labeled α-GFP^{ATTO655} fNbs. The grey and red lines represent absorption at 280 nm (A280) and ATTO655 fluorescence at $\lambda_{ex/em}$ 655/680 nm.

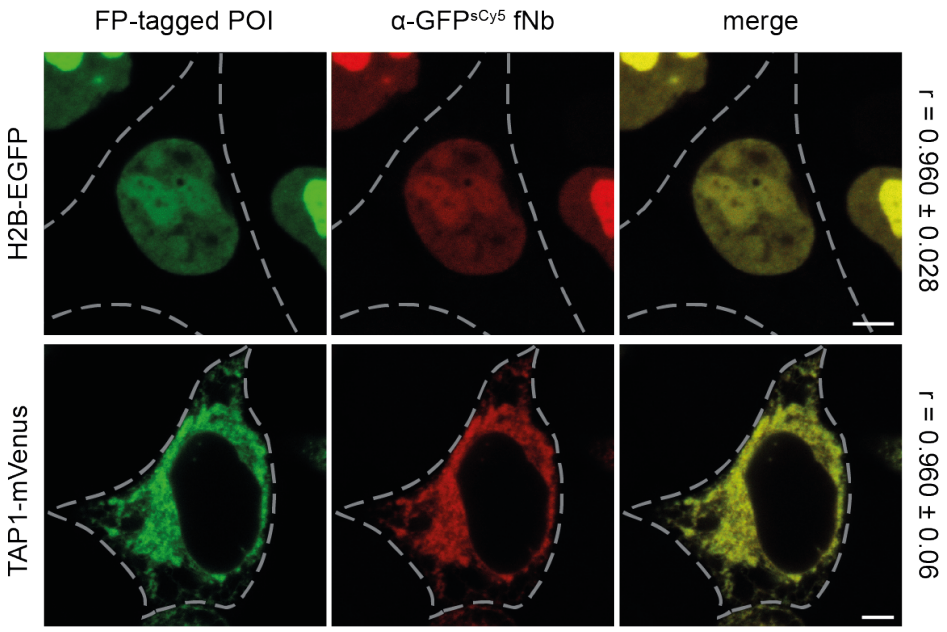

Figure S3. Specific binding of site-specifically labeled α-GFP^{sCy5} fNbs.

HeLa Kyoto cells expressing H2B^{EGFP} or TAP1^{mVenus} (green) were fixed with 4% formaldehyde and labeled with 100 nM of α-GFP^{sCy5} fNb (red). Excellent co-localization (merge) between the fNbs and both FP-tagged POIs was detected. Pearson's coefficients (r) were calculated from 9-11 individual cells (right). Dashed lines indicate the cell border. Scale bar: 5 µm.

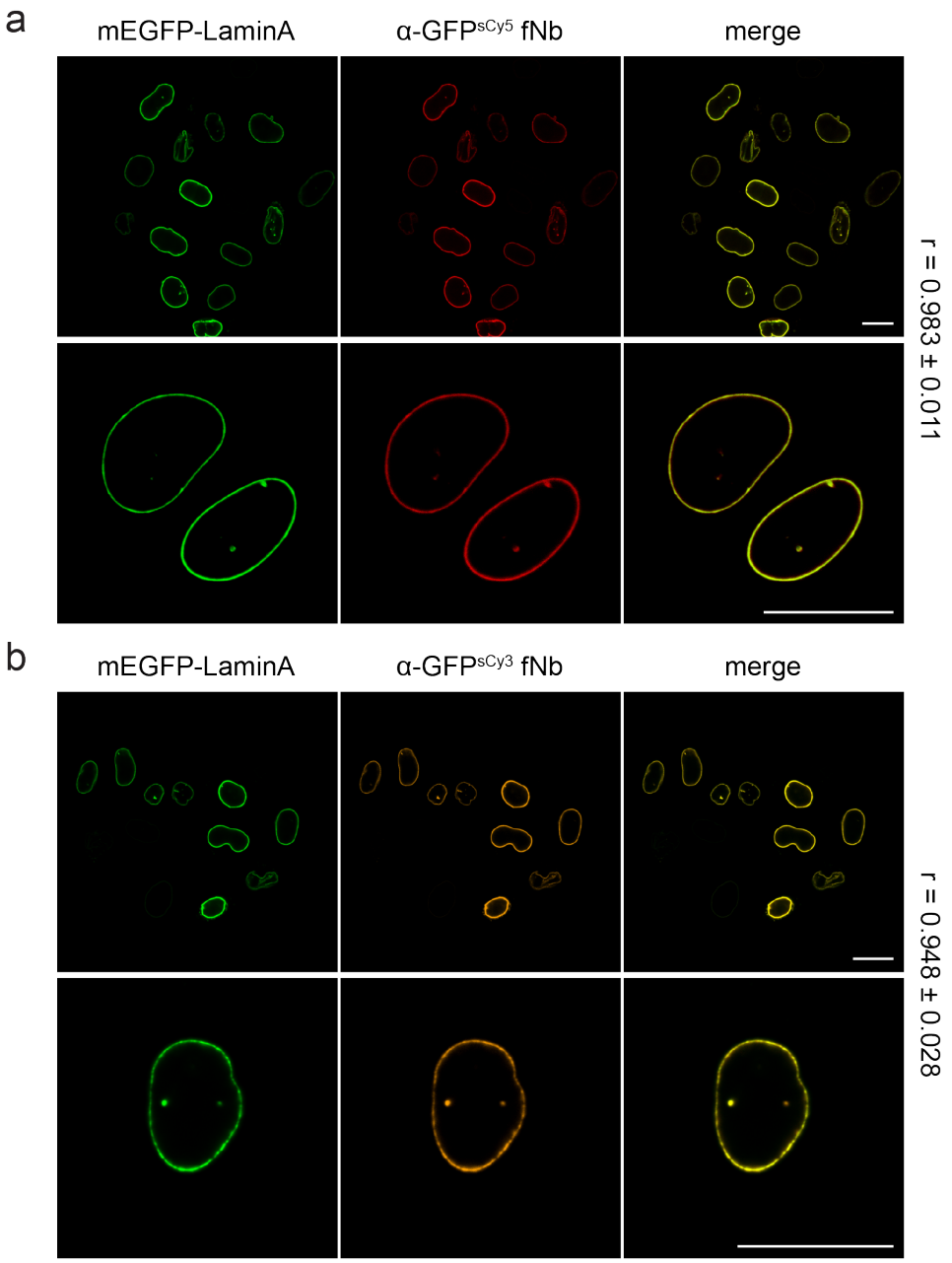

Figure S4. Specific labeling of mEGFP-Lamin A with α-GFP^{sCy3} and α-GFP^{sCy5} fNbs.

After fixation and permeabilization, HeLa Kyoto cells expressing mEGFP-Lamin A were labeled with 100 nM of α-GFP^{sCy5} (**a**) or α-GFP^{sCy3} fNbs (**b**) and analyzed *via* CLSM. mEGFP-Lamin A was specifically labeled by the fNbs with very low background and the staining intensity correlated with the POI´s expression level. Scale bars: 20 µm.

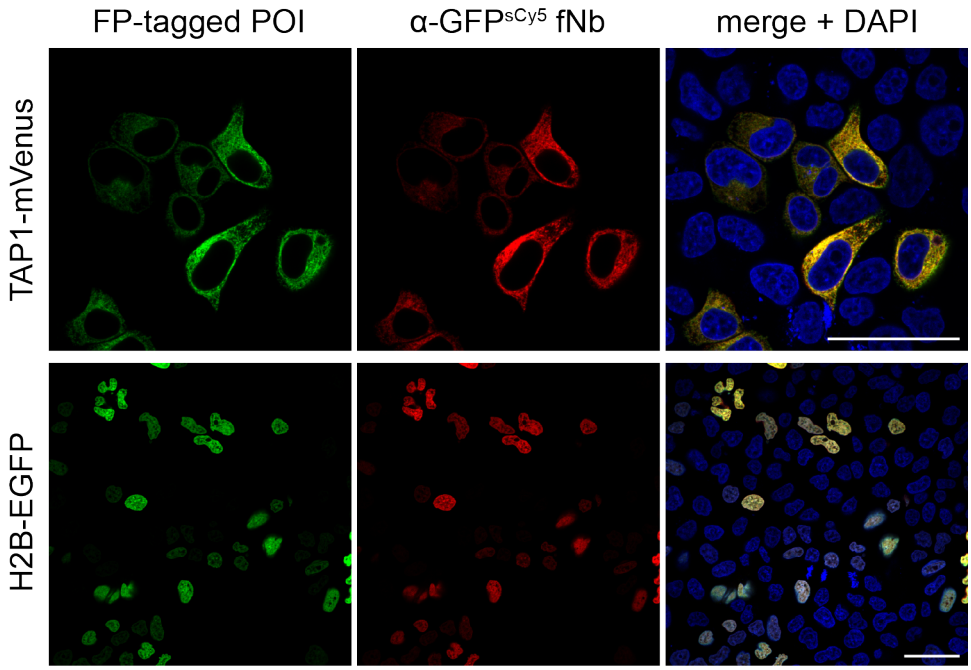

Figure S5. Expression levels of target proteins correlate with the labeling density of the α-GFP fNbs.

After fixation and permeabilization, HeLa Kyoto cells expressing TAP1^{mVenus} or H2B^{EGFP} were stained with α-GFP^{sCy5} fNbs (50 nM). The labeling intensity highly correlates with the expression level of both FP-fused POIs, reflecting stoichiometric target decoration. Imaging was performed by CLSM. Scale bars: 50 µm.

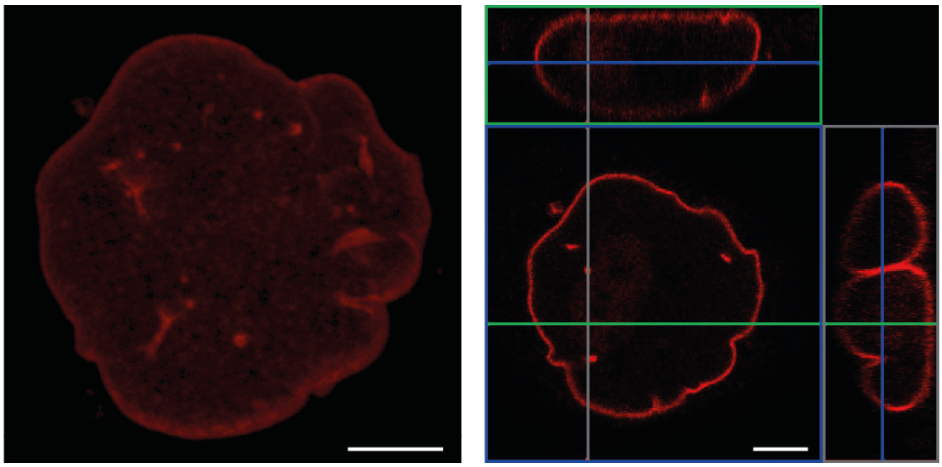

Figure S6. Specific labeling of endogenous nuclear envelope with α-Lamin^{ATTO655}.

After fixation, the endogenous nuclear lamina of HeLa Kyoto cells was visualized by 100 nM of α-Lamin^{ATTO655} fNb (red). 3D reconstruction of a z-stack showed a dense labeling of the nuclear lamina along with a high signal-to-background ratio (see Supplemental Video 1). Images were taken by CLSM with the Airy Scan detector. Scale bars: 5 µm.

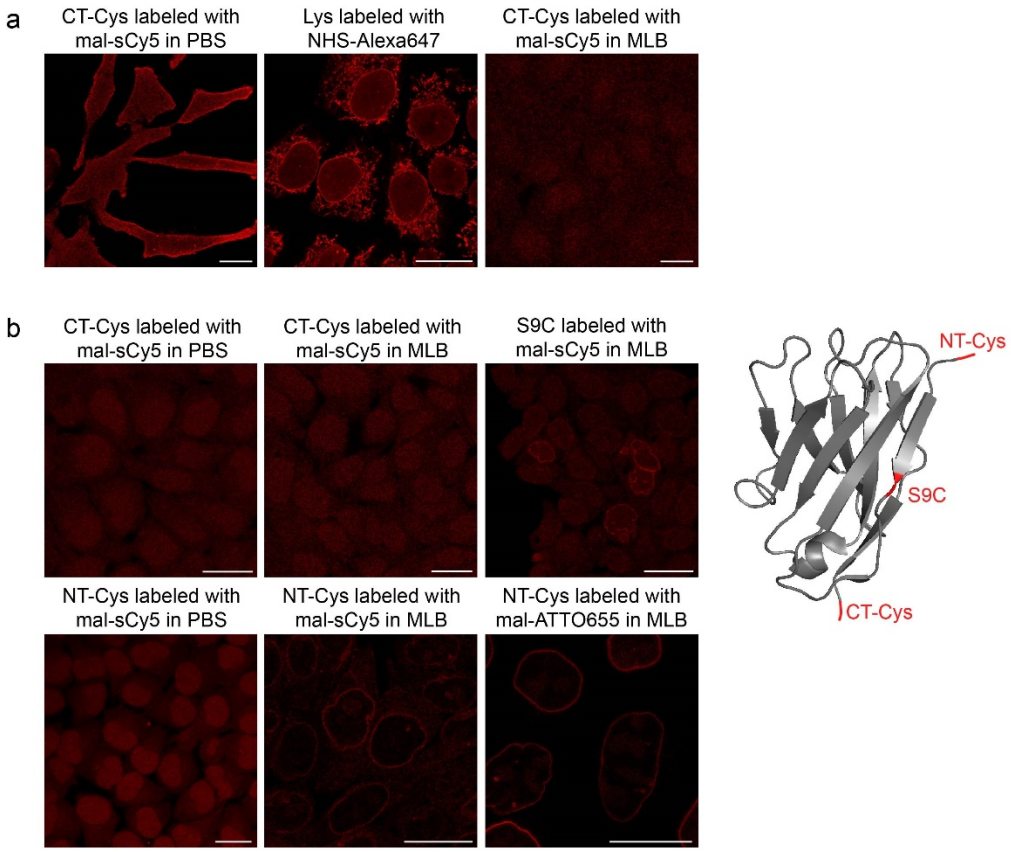

Figure S7. Labeling screen of differently modified α-Lamin fNbs.

The α-Lamin nanobody was engineered with an extra single cysteine at three different positions, *e.g.* N-terminally (NT-Cys), C-terminally (CT-Cys), or at position 9 (S9C). After production in *E. coli* BL21/DE3 (**a**) or *E. coli* T7 SHuffle Express (**b**) and affinity purification, the engineered nanobodies were modified with maleimide sCy5 or ATTO655. Stochastic labeling via lysines exposed on the nanobody surface was conducted with NHS Alexa647. The specificity of these fNbs was evaluated by staining of HeLa Kyoto cells (500 nM) after fixation and permeabilization. fNb target specificity was analyzed by CLSM. For the CT-Cys labeled, S9C labeled and Lys labeled fNbs a severe lack in target specificity was observed. After production in *E. coli* T7 SHuffle Express and subsequent modification of the N-terminal cysteine in maleimide labeling buffer (MLB), specific tracing of endogenous lamin was achieved with greatly enhanced signal-to-background ratio. This fNb format was used for all further experiments. Scale bars: 20 µm.

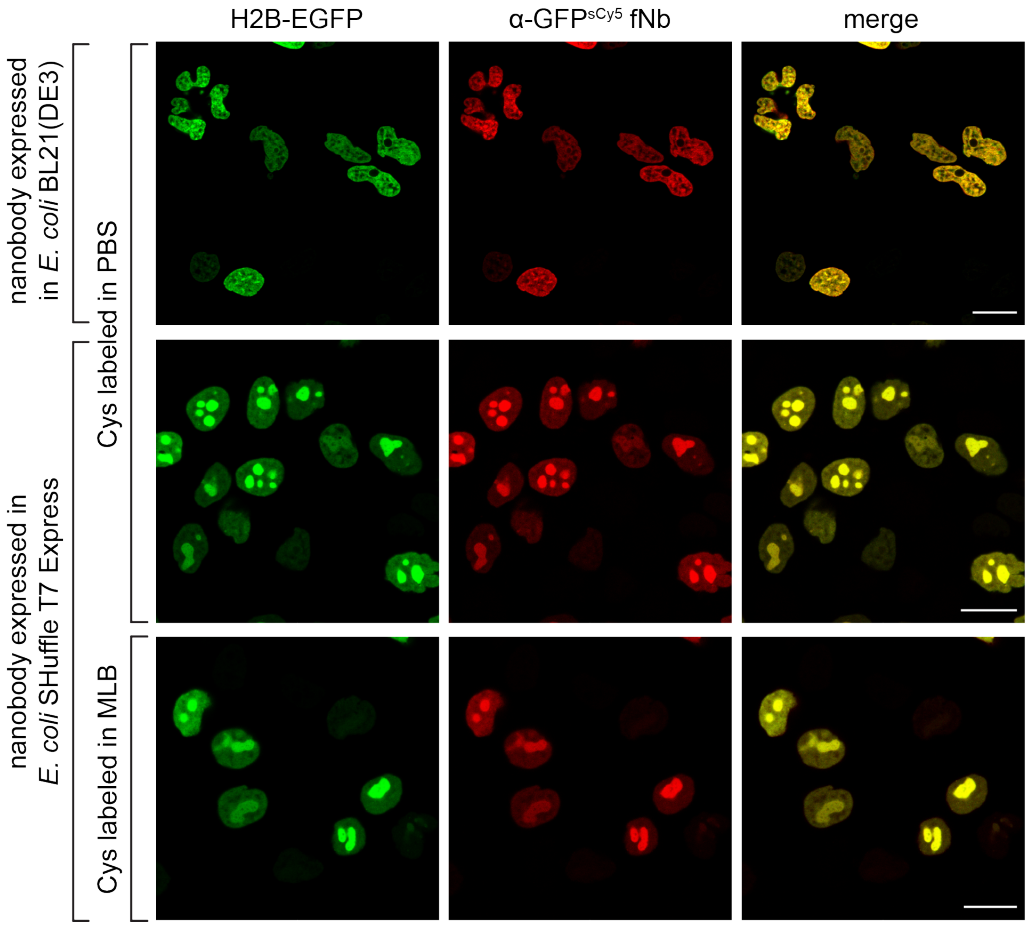

Figure S8. Labeling screen of differently prepared α-GFP fNbs.

The α-GFP^{sCy5} fNb with an N-terminal cysteine was produced in two different *E. coli* strains (BL21/DE3 or T7 SHuffle Express), and modified with maleimide sCy5. α-GFP binding screen was performed against H2B^{EGFP} (green) for all tested fNb preparation conditions. Fixed and permeabilized HeLa Kyoto cells were stained with α-GFP^{sCy5} fNb (100 nM, red). All combinations for fNb generation resulted in specific labeling of H2B^{EGFP} (merge) by the engineered α-GFP with low background labeling. Analysis was performed by CLSM. Scale bars: 20 µm.

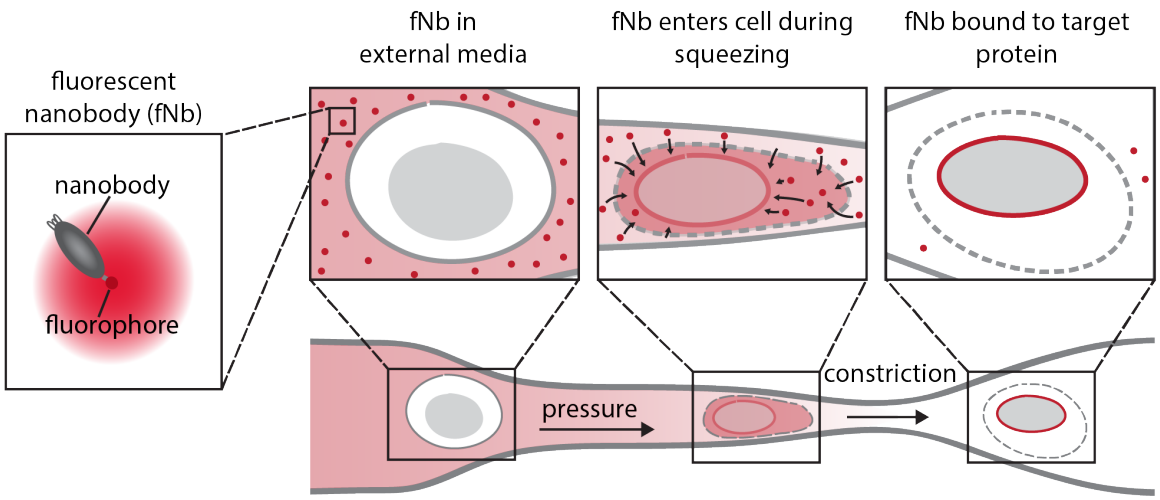

Figure S9. Nanobody transfer into living cells by microfluidic cell squeezing.

Cells are pressed through constrictions, which are ~ 30% smaller than cell diameter. Shear forces cause the formation of transient holes in the plasma membrane. By passive diffusion (middle), site-specifically labeled fNbs enter the cytosol and bind to their target (right, binding to nuclear envelope is exemplarily illustrated). The induced holes reseal within ~ 5 min.

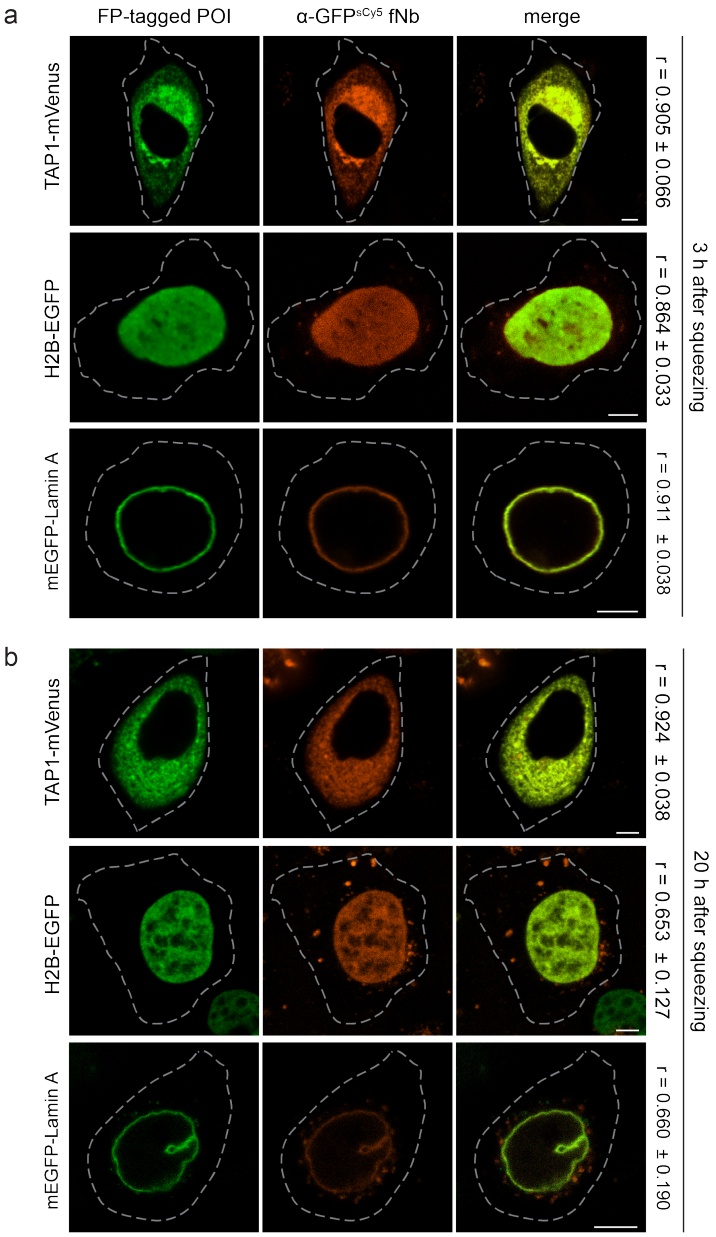

Figure S10. Live-cell labeling of FP-tagged targets via α-GFP^{sCy3} fNbs.

α-GFP^{sCy3} fNb (200 nM) was transferred into HeLa Kyoto cells transiently transfected with TAP1^{mVenus}, H2B^{EGFP}, or ^{mEGFP}Lamin A, respectively. Cells were imaged 3 h (**a**) and 20 h (**b**) after cell squeezing by CLSM. For all tested subcellular localizations of the FP-tagged POI, the molecular specificity of the fNb was persistent for a prolonged period of time (20 h). After 20 h, background originating as cytosolic punctae was detected. This observation is supported by a decreased Pearson´s coefficient (r, right), calculated from 8-10 individual cells. Dashed lines indicate the cell border. Scale bars: 5 µm.

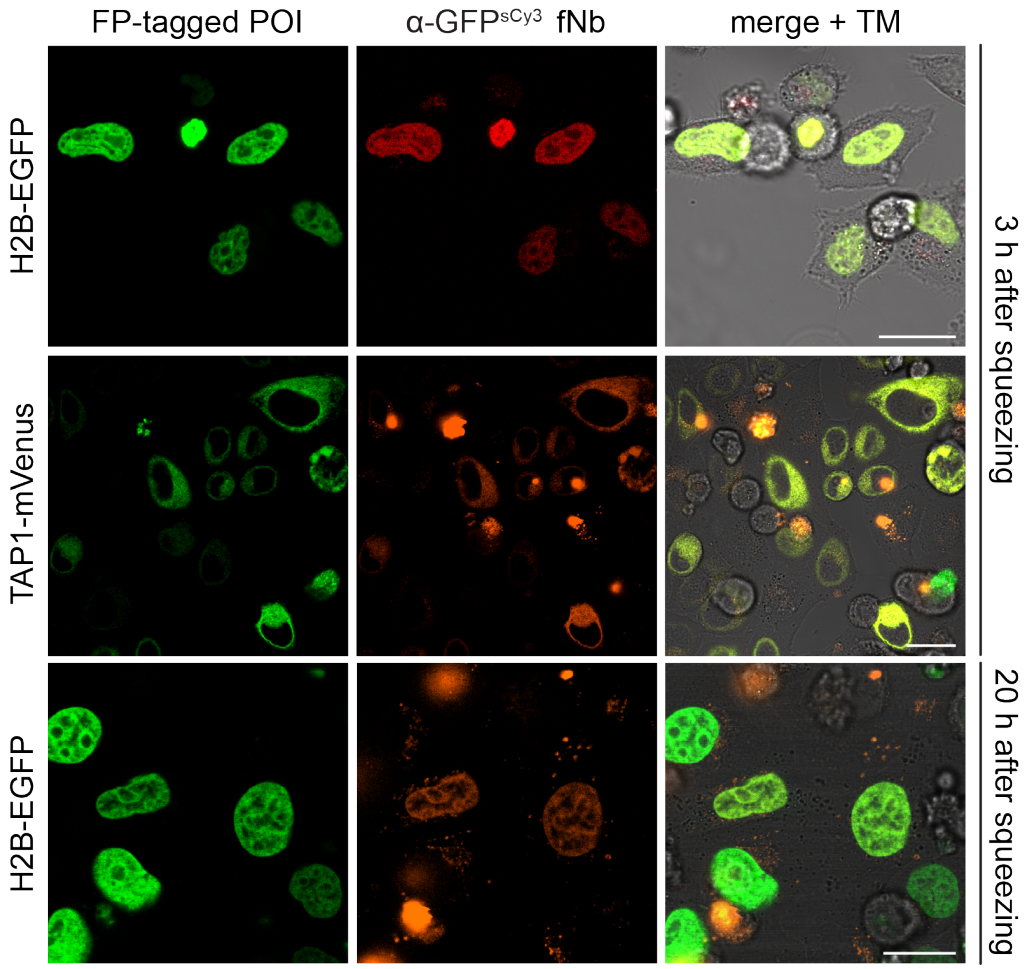

Figure S11. Fluorescence correlation of target proteins and α-GFP^{sCy3} fNb in living cells.

HeLa Kyoto cells expressing TAP1^{mVenus} or H2B^{EGFP} (green) were squeezed in the presence of α-GFP^{sCy3} fNb (200 nM, orange). Imaging via CLSM was performed 3 h and 20 h after squeezing. Low background and high co-localization between the fNb and POI was observed in multiple cells with varying expression level. Incipient punctual background was detectable after 20 h (bottom). Scale bars: 20 µm.

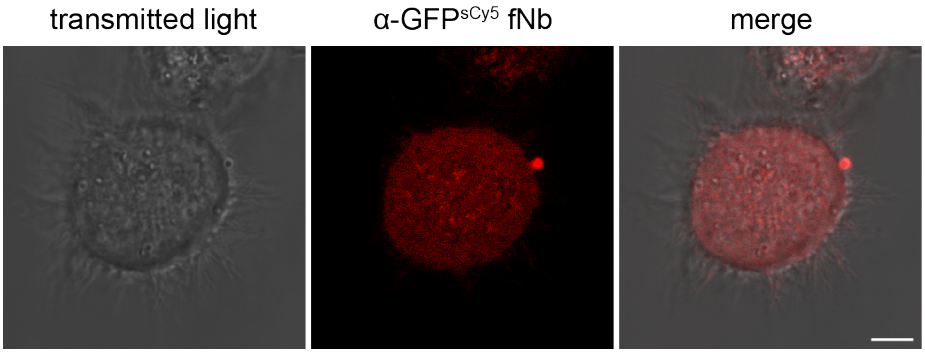

Figure S12. Distribution of α-GFP^{sCy5} fNbs in untransfected, GFP-negative cells.

α-GFP^{sCy5} fNb (100 nM) was delivered into HeLa Kyoto cells via cell squeezing. A cytosolic distribution of the fNb (red) was detected 1 h after squeezing. In absence of FP-tagged proteins, no distinct cellular localization of α-GFP^{sCy5} fNbs was observed, confirming the molecular specificity of the α-GFP^{sCy5} fNb for antigen tracking. Imaging was performed by CLSM. Scale bar: 5 µm.

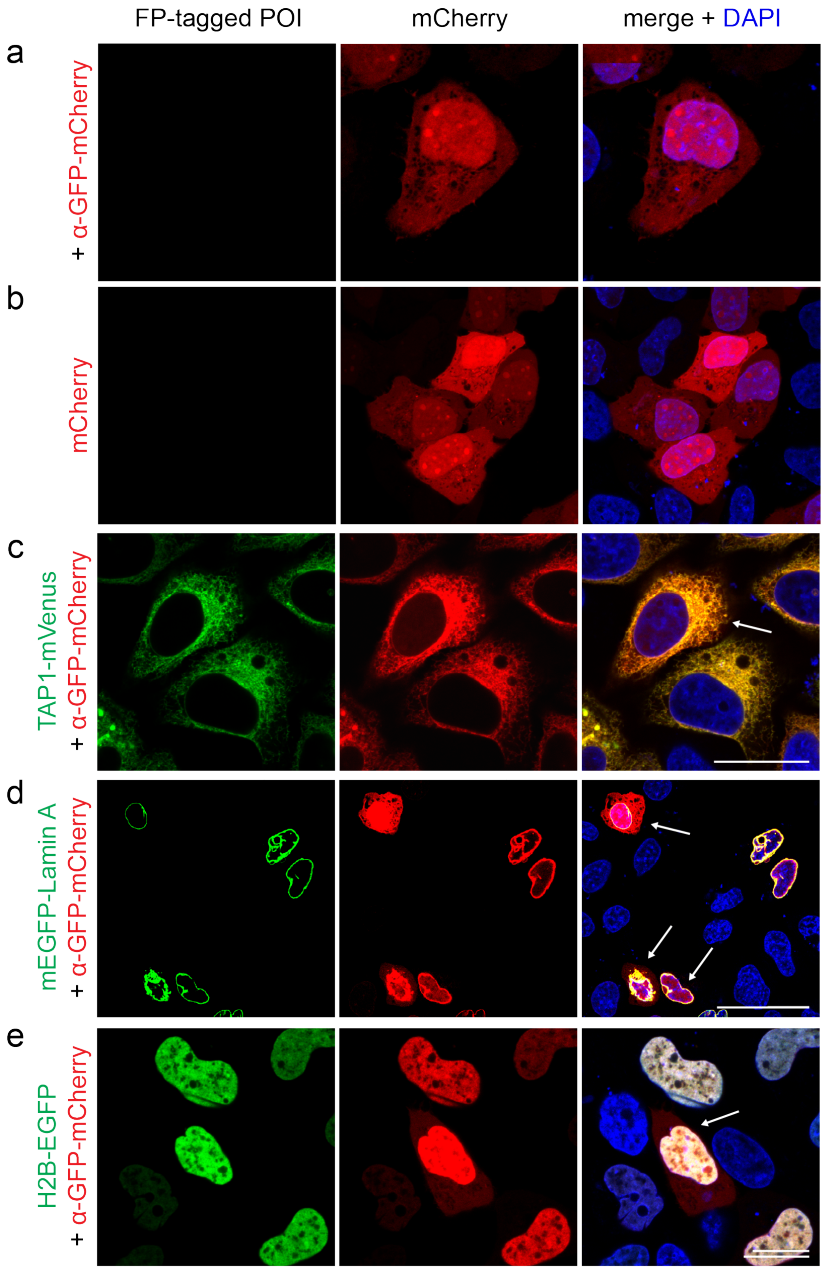

Figure S13. Transient expression of α-GFP-mCherry chromobody in mammalian cells.

(**a**) In the absence of the target protein, the α-GFP-mCherry nanobody was homogenously distributed within the cytosol and nucleus, similar to mCherry alone (**b**). (**c**-**e**) HeLa Kyoto cells were transiently co-transfected with an α-GFP-mCherry chromobody (red) and a FP-tagged POI, *e.g.* TAP1^{mVenus}, ^{mEGFP}Lamin A or H2B^{EGFP} (green). Increased chromobody expression levels resulted in a high background of unbound nanobody, distributed in the cytosol and nucleus (indicated by arrows). Before CLSM imaging, HeLa Kyoto cells were chemically arrested with 4% formaldehyde and additionally stained with DAPI (blue). Scale bars: 20 µm.

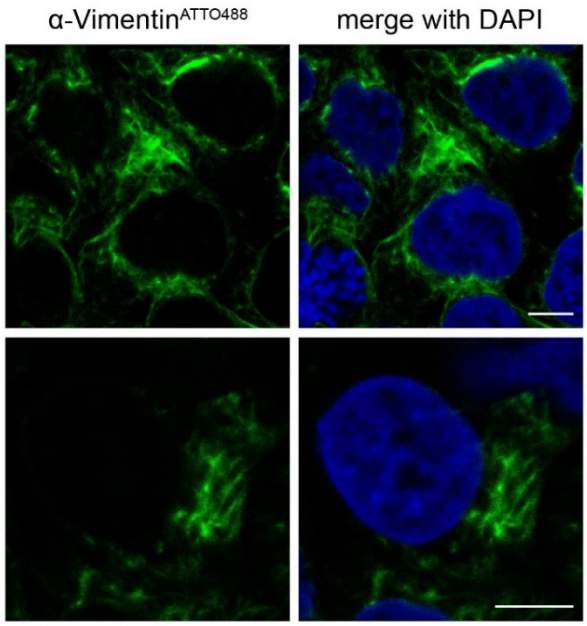

Figure S14. Vimentin staining in fixed cells.

HeLa Kyoto cells were fixed, permeabilized and stained with α-Vimentin^{ATTO488} (20 µg/ml, green) and DAPI (blue). Confocal imaging showed specific labeling of endogenous filamentous vimentin. Scale bars: 5 µm.

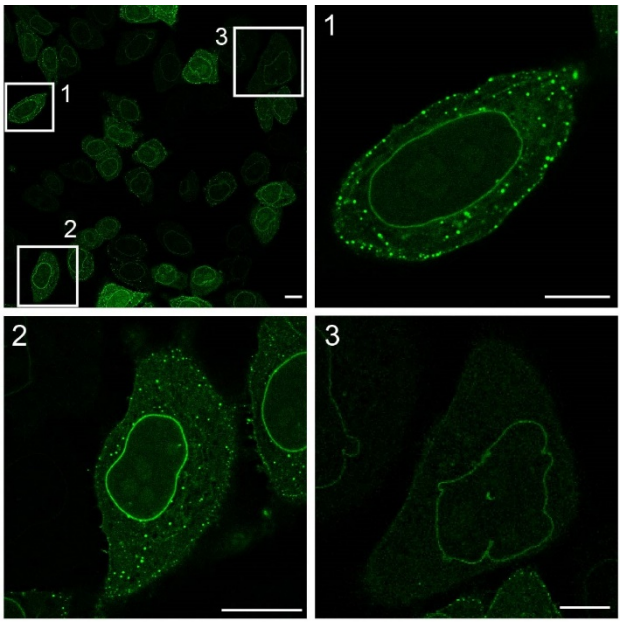

Figure S15. Transient expression of α-Lamin-EGFP chromobody in HeLa Kyoto cells entails background of free nanobody.

Cells transiently transfected with α-Lamin-EGFP were fixed with 4% formaldehyde 24 h after transfection. Specific decoration of endogenous lamin at the nuclear envelope was visualized by CLSM. The variability of the chromobody expression level was accompanied by a high background, originating as cytosolic punctae. Images 1-3 are magnifications of individual cells as indicated by white boxes in the upper left image. Scale bars: 10 µm.

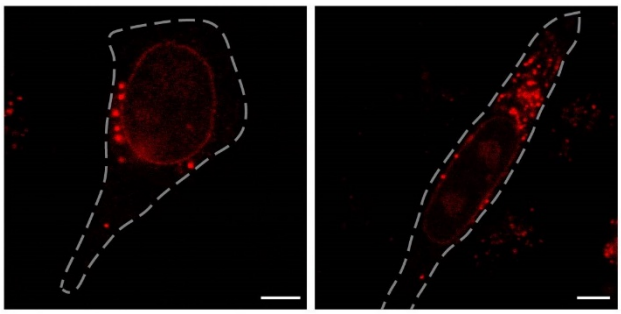

Figure S16. Persistence of endogenous lamin targeting by fNbs in living cells.

The α-Lamin^{sCy5} fNb (500 nM) was transferred into native HeLa Kyoto cells via cell squeezing. Specific decoration of the endogenous nuclear lamina by fNbs was still observed 20 h after squeezing by CLSM. An enriched punctual background was detected compared to 3 h post squeezing (see Fig. 3a). Dashed lines indicate the cell border. Scale bars: 5 µm.

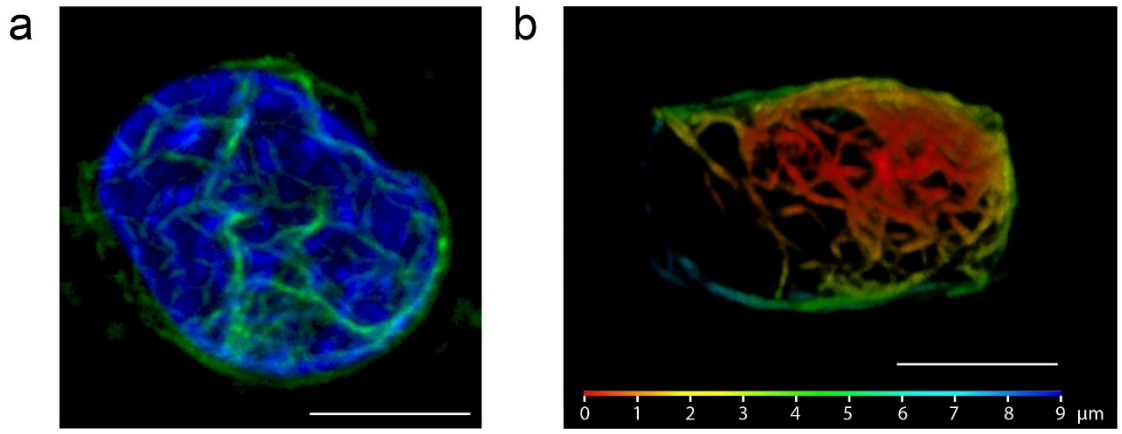

Figure S17. 3D reconstruction of endogenous vimentin network.

After intracellular transfer of α-Vimentin^{ATTO488} (50 µg/ml), z-stacks were recorded by confocal imaging using the Airy scan detector (SR mode, Zeiss). (**a**) Imaging was performed 3 h after squeezing with additional HOECHST staining (blue). The 3D reconstruction of the obtained z-stack showed the complex network of endogenous vimentin (green), organized around nucleus. (**b**) 3D topographic map of the endogenous vimentin meshwork. The series of z-stacks was recorded 20 h after cell squeezing and reconstructed. The rainbow-color code indicates the depth. Distance between stacks: ~ 200 nm, respectively. Scale bars: 5 µm.

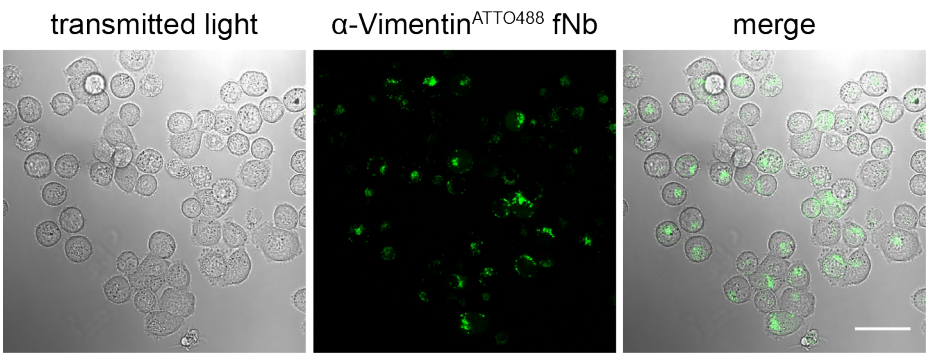

Figure S18. Transduction efficiency of α-Vimentin^{ATTO488} fNbs in untransfected cells.

The α-Vimentin^{ATTO488} fNb was transferred into native HeLa Kyoto cells via cell squeezing. Successful fNb delivery in multiple cells simultaneously was observed, demonstrating the high transduction efficiency of the cell squeezing approach. Imaging was performed 1 h after squeezing by CLSM. Scale bars: 20 µm.

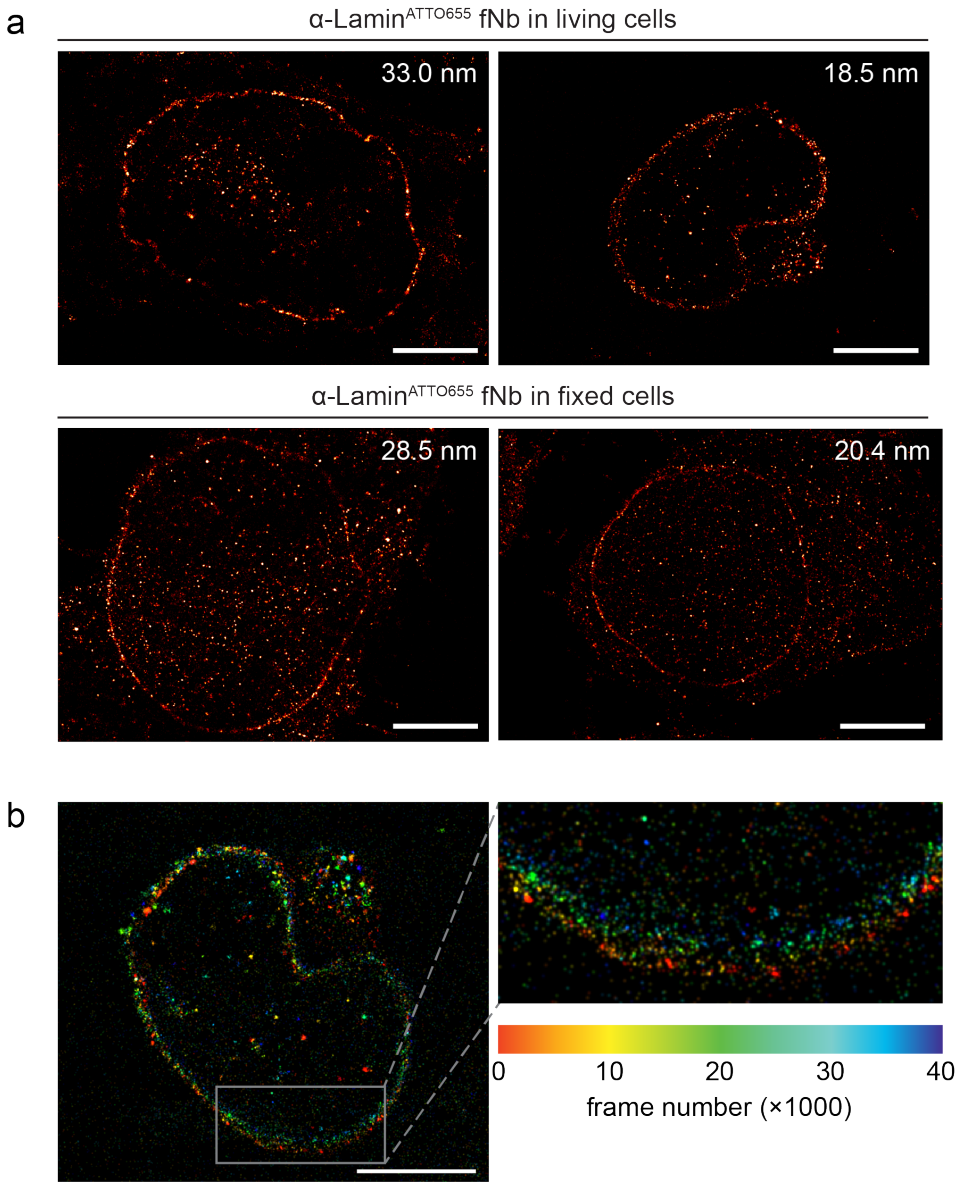

Figure S19. Super-resolution imaging of endogenous lamin in fixed and in living cells. HeLa Kyoto cells were either squeezed with α-Lamin^{ATTO655} fNb (500 nM) for live-cell imaging or fixed, permeabilized and stained with α-Lamin^{ATTO655} fNb (100 nM). (**a**) *d*STORM analysis revealed a similar average localization precision in living (23.4 ± 8.3 nm, top) and fixed (23.2 ± 4.6 nm, bottom) cells. The localization precision determined for each image is given in the top right corner. Mean and standard deviation were calculated from three images. (**b**) Cell dynamics during live-cell super-resolution microscopy can impede imaging. Frame numbers are color-coded. Scale bars: 5 µm.

Supplemental Video 1 I 3D reconstruction of the endogenous nuclear lamina.

After fixation and permeabilization, endogenous lamin of a HeLa Kyoto cell was visualized with an α-Lamin^{ATTO655} (100 nM). 53 individual stacks were recorded by confocal imaging using the Airy scan detector (Zeiss, distance between stacks ~ 200 nm). 3D reconstruction showed a dense decoration of the complete nuclear lamina by the fNb, accompanied with a high signal-to-background ratio. Several intranuclear structures of endogenous lamin were observed.

Supplemental References

Endesfelder, U., Malkusch, S., Fricke, F., and Heilemann, M. (2014). A simple method to estimate the average localization precision of a single-molecule localization microscopy experiment. Histochem Cell Biol *141*, 629-638.

Girish, V., and Vijayalakshmi, A. (2004). Affordable image analysis using NIH Image/ImageJ. Indian J Cancer *41*, 47.

Kirchhofer, A., Helma, J., Schmidthals, K., Frauer, C., Cui, S., Karcher, A., Pellis, M., Muyldermans, S., Casas-Delucchi, C.S., Cardoso, M.C*., et al.* (2010). Modulation of protein properties in living cells using nanobodies. Nat Struct Mol Biol *17*, 133-138.

Kollmannsperger, A., Sharei, A., Raulf, A., Heilemann, M., Langer, R., Jensen, K.F., Wieneke, R., and Tampé, R. (2016). Live-cell protein labelling with nanometre precision by cell squeezing. Nat Commun *7*, 10372.

Malkusch, S., and Heilemann, M. (2016). Extracting quantitative information from single-molecule super-resolution imaging data with LAMA – LocAlization Microscopy Analyzer. Sci Rep *6*, 34486.

Parcej, D., Guntrum, R., Schmidt, S., Hinz, A., and Tampé, R. (2013). Multicolour fluorescence-detection size-exclusion chromatography for structural genomics of membrane multiprotein complexes. PLoS One *8*, e67112.

Schindelin, J., Arganda-Carreras, I., Frise, E., Kaynig, V., Longair, M., Pietzsch, T., Preibisch, S., Rueden, C., Saalfeld, S., Schmid, B*., et al.* (2012). Fiji: an open-source platform for biological-image analysis. Nat Methods *9*, 676-682.

Uphoff, C.C., and Drexler, H.G. (2014). Detection of mycoplasma contamination in cell cultures. Curr Protoc Mol Biol *106*, 28 24 21-28 24 14.

Wolter, S., Schuttpelz, M., Tscherepanow, M., S, V.D.L., Heilemann, M., and Sauer, M. (2010). Real-time computation of subdiffraction-resolution fluorescence images. Journal of microscopy *237*, 12-22.